Journal of Medicinal Chemistry Article

*J. Med. Chem.* **2011,** *54,* 719–733 **719**
DOI: 10.1021/jm101317f

# Modeling Cellular Pharmacokinetics of 14- and 15-Membered Macrolides with Physicochemical Properties

Višnja Stepanić,[†,§] Sanja Koštrun,[†,∥] Ivica Malnar,[†,∥] Mario Hlevnjak,[†,⊥] Kristina Butković,[†,∥,▽] Irena Ćaleta,[†,∥,▽] Marko Dukši,[†,∥,▽] Goran Kragol,[†,∥,▽] Oresta Makaruha-Stegić,[#,▽] Lara Mikac,[†,×,▽] Jovica Ralić,[†,∥,▽] Iva Tatić,[†,∞,▽] Branka Tavčar,[†,∥,▽] Klara Valko,[‡,▽] Selvira Zulfikari,[●,▽] and Vesna Munić*[,†,∥]

[†]*GlaxoSmithKline Research Centre Zagreb Ltd., Prilaz baruna Filipovića 29, HR-10000 Zagreb, Croatia, and* [‡]*Analytical Chemistry, Molecular Discovery Research, GlaxoSmithKline, Gunnels Wood Road, Stevenage, Herts SG1 2NY, U.K.* [§] *Present address: Laboratory for Epigenomics, Division of Molecular Medicine, Ruđer Bošković Institute, Bijenička 54, HR-10000 Zagreb, Croatia.* [∥] *Present address: Galapagos istraživački centar d.o.o. Ltd, Prilaz baruna Filipovića 29, HR-10000 Zagreb, Croatia.* [⊥] *Present address: Laboratory of Computational Biophysics, Mediterranean Institute for Life Sciences, Meštrovićevo šetalište bb, HR-21000 Split, Croatia.* [#] *Axellia Pharmaceuticals—Branch Zagreb, Radoslava Cimermana 40, HR-10000 Zagreb, Croatia.* [×] *Present address: Molecular Physics Laboratory, Division of Materials Physics, Ruđer Bošković lnstitute, Bijenička 54, HR-10000 Zagreb, Croatia.* [∞] *Present address: Bijenik 24, HR-10000 Zagreb, Croatia.* [●]*Agency for Medicinal Products and Medical Devices, Ksaverska 4, HR-10000 Zagreb, Croatia.* [▽]*These authors are listed in alphabetical order.*

*Received May 29, 2010*

Macrolides with 14- and 15-membered ring are characterized by high and extensive tissue distribution, as well as good cellular accumulation and retention. Since macrolide structures do not fit the Lipinski rule of five, macrolide pharmacokinetic properties cannot be successfully predicted by common models based on data for small molecules. Here we describe the development of the first models for macrolide cellular pharmacokinetics. By comparison of cellular accumulation and retention in six human primary cell cultures of leukocytic and lung origin, as well as in lung carcinoma cell line NCI-H292, this cell line was found to be an adequate representative cell type for modeling macrolide cellular pharmacokinetics. Accumulation and retention in the NCI-H292 cells, as well as various physicochemical properties, were determined for a set of 48 rationally designed basic macrolide compounds. Classification models for predicting macrolide cellular accumulation and retention were developed using relatively easily determined and conceptually simple descriptors: experimentally determined physicochemical parameters ChromlogD and CHI IAM, as well as a calculated number of positively charged atoms (POS). The models were further tested and improved by addition of 37 structurally diverse macrolide molecules.

## Introduction

Macrolides with 14- and 15-membered polyketide ring are a very well established class of antimicrobial compounds widely used in clinics. The first member of the class was erythromycin A, isolated in 1952 from the actinomycete *Saccharopolyspora erythraea*. Several semisynthetic macrolides followed, with azithromycin being the most successful on the market.[1] In past decades there have been a number of reports describing other properties of macrolide class, like anti-inflammatory/immunomodulatory,[2,3] antitumor,[4,5] antiviral, and antimalarial.[6,7] Anti-inflammatory activities have received the most attention. So far the best activities have been observed in chronic inflammatory diseases with dominant neutrophilic infiltration, where macrolides inhibit accumulation of neutrophils in inflamed tissues, as well as proinflammatory cytokine release. Nowadays, macrolides are used in the treatment of diffuse panbronchiolitis and cystic fibrosis, and their potential applications in chronic obstructive pulmonary disease, chronic sinusitis, asthma, bronchiectasis, and bronchiolitis obliterans have also been reported.[8]

A part of the success of macrolides as drugs is due to their distinct PK[a] properties. Macrolides highly accumulate in cells and tissues. Their concentrations in tissues are often 10- to 100-fold higher than those found in plasma, depending on the macrolide and the tissue studied. It is also well documented that macrolides accumulate in cells in vitro. During 3 h of incubation with cells some macrolides can reach intracellular concentrations up to 500-fold higher than extracellular concentrations.[9−12] There have been many reports on cellular uptake and release of the most frequently used macrolide antibiotics in different cell types,[9,10] and the intensity of cellular accumulation was found to differ depending on the cell type. Phagocytic cells have often been reported to highly

*To whom correspondence should be addressed. Address: Galapagos istraživački centar d.o.o. Ltd., Prilaz baruna Filipovića 29, HR-10000 Zagreb, Croatia. Phone: 385 1 8886323. Fax: 385 1 8886443. E-mail: vesna.munic@glpg.com.

[a] Abbreviations: ACC, accumulation; Azi, azithromycin; BSMC, bronchial smooth muscle cells; CHI, chromatographic hydrophobicity index; compd, compound; IAM, immobilized artificial membrane; MDM, monocyte derived macrophage; NCI-H292, a lung carcinoma cell line; NHBE, normal human bronchial epithelial cells; NHLF, normal human lung fibroblasts; PBS, phosphate buffered saline; PCA, principal component analysis; pCF, negative logarithm of the fraction of singly charged molecules; PD, pharmacodynamic; PERM, artificial membrane permeability; PK, pharmacokinetic; PLS, partial least squares; PMN, polymorphonuclear leukocytes; pNF, negative logarithm of the fraction of neutral molecules; POS, number of positively charged centers; RET, retention; SD, standard deviation; Sol, solubility; TLy, T-lymphocytes; TP, total proteins.



Published on Web 01/05/2011

accumulate macrolides, which is largely due to the fact that 40−60% of cell-associated macrolide is found in acidic cellular compartments, such as lysosomes or azurophil granules of polymorphonuclear leukocytes, where they are considered to be trapped by protonation.[10,13−15] Upon removal of the drug from the extracellular milieu, the trapped drug is slowly released.[14]

Such affinity for cells ensures them large volume of distribution ($V_{dss}$) in vivo, and high cellular retention results in prolonged half-life ($t_{1/2}$) in blood and tissues, enabling a more favorable dosing regimen (e.g., only $3 \times 500$ mg/day is a standard dose for azithromycin).[16,17] High intracellular concentrations of macrolides enable them better penetration to intracellular pathogens (e.g., *Clamydia, Legionella*) and other putative intracellular targets, as well as prolonged presence in the inflammatory cells.[16,17]

In order to expand the possibilities of using macrolides as a new class of anti-inflammatory drugs, new macrolide derivatives with PK/PD properties adequate for new indications will need to be developed.

Although macrolides are not fully Lipinski compliant molecules, marketed macrolides with 14- and 15-membered ring possess two key properties of successful drugs: $\log P \leq 5$ and number of hydrogen bond donors is ≤5. According to Ganesan's proposal[18] of two classes of successful natural product leads, macrolides thus fit into the "parallel universe" of successful natural products, compounds that do not fit into most of the criteria for druglikeness apart from the two mentioned. However, with Mw > 700 and a number of hydrogen bond acceptors of > 10, macrolide structures do not fit into Lipinski rule of five nor several other drug-likeness criteria. Their PK properties hence cannot be successfully predicted by standard models built on data sets of small molecules.[19,20] For example, most macrolide derivatives with 14- and 15-membered ring fall into the same group of basic molecules with Mw > 700 and $\log P$ mainly ranging from 3 to 5, as defined by Gleeson.[19] Similarly, physicochemical properties like $\log P$ cannot be accurately calculated for macrolides by available programs.[21] Since relatively minor structural modifications can cause a significant change in macrolide PK properties,[22] a more detailed analysis of molecular characteristics critical for PK behavior of compounds within macrolide class is necessary.

While the literature mainly reports cellular accumulation and retention data for several marketed antimicrobial macrolides, to our knowledge larger screens of macrolide cellular accumulation and retention have not been conducted so far. Here, we present representative NCI-H292 cell based assay for a systematic screen of a larger number of macrolide derivatives in cellular accumulation and retention studies. Additionally, computational classification models for predicting macrolide cellular pharmacokinetics were developed using relatively easily determined and conceptually simple descriptors: experimentally determined physicochemical parameters ChromlogD (rescaled CHI[23]), CHI IAM,[24] and a calculated number of positively charged atoms (POS). Such models are preferable in the case of macrolides since, because of their complex structure, calculation of 3D descriptors is time-consuming and not applicable for larger number of compounds and available force fields are not able to reliably reproduce conformations of macrocyclic ring and flexible substituents.

## Results and Discussion

**Design of Training and Validation Sets.** The study was performed in consecutive steps with the following four compound sets:

(1) Initial set of eight representative compounds was designed to span a wide property space in terms of lipophilicity (measured as $\log P_{o/w}$) and cellular PK (measured as accumulation and retention in widely used phagocytic cells, PMNs). It was used to extensively study accumulation and retention in a series of primary human cell cultures. The initial set consisted of macrolide antibiotics clarithromycin and azithromycin, their 9a-lactam analogue, and derivatives of these three macrolides (Figure 1a).

(2) Training set used for building models for accumulation and retention in lung epithelial NCI-H292 cells contained 30 compounds: 8 from the initial set (Figure 1a), 3 additional macrolide antibiotics (erythromycin A (cpd 28), roxithromycin (cpd 29), and tylosin (cpd 30)), and 19 new rationally designed macrolides obtained by attaching a few structurally simple, neutral heteroalkyl chains at various positions of azithromycin or clarithromycin scaffolds (Figure 1b).

(3) Validation set consisted of 18 new macrolides synthesized using an analogous approach as for the creation of the training set (Figure 1c). In addition to azithromycin and clarithromycin, 9a-lactam and oxime scaffolds were also explored.

(4) An extended set of macrolides consisted of all 48 molecules of training and validation sets, with the additional 37 macrolides synthesized within a drug discovery research program on novel anti-inflammatory macrolides. The extended set was used to additionally test the applicability of the obtained models for more diverse compounds. Apart from adding diverse substituents to 14- and 15-membered macrolide rings, some of the compounds additionally included chemical modifications such as rearrangements of macrolactone or sugar rings and/or various substitutions at the desosamine nitrogen atom.

**Cellular Accumulation and Retention in Six Human Primary Cell Types and Cell line NCI-H292.** Because macrolides reach very high concentrations in lungs and because their anti-inflammatory activity was mostly reported for respiratory diseases, we have determined the accumulation and retention of the eight macrolide compounds (Figure 1a) in six human primary cell cultures of lung and leukocyte origin: bronchial epithelium (NHBE), bronchial smooth muscle cells (BSMC), lung fibroblasts (NHLF), polymorphonuclear leukocytes (PMN), T-lymphocytes (TLy), monocyte derived macrophages (MDM), and lung carcinoma cell line NCI-H292.

To compare absolute accumulation intensities of a reference macrolide azithromycin in different cell types, the amount of azithromycin accumulated in cells after 3 h of incubation at 10 $\mu$M was normalized to total protein (TP) content in samples. Obtained concentrations of azithromycin (±SD) were $56.5 \pm 37.2$, $9.4 \pm 4.1$, $8.9 \pm 3.0$, $9.8 \pm 0.6$, $4.7 \pm 1.3$, $3.7 \pm 1.8$, and $3.3 \pm 0.9$ nmol/mg TP for BSMC, MDM, PMN, NCI-H292, NHBE, TLy, and NHLF, respectively. Although the absolute values showed a rather large variation between experiments (most probably due to inter-individual differences between donors), the relative ratios between the compounds remained the same. As our primary focus was to compare macrolides among themselves, the cellular accumulations of tested compounds were expressed

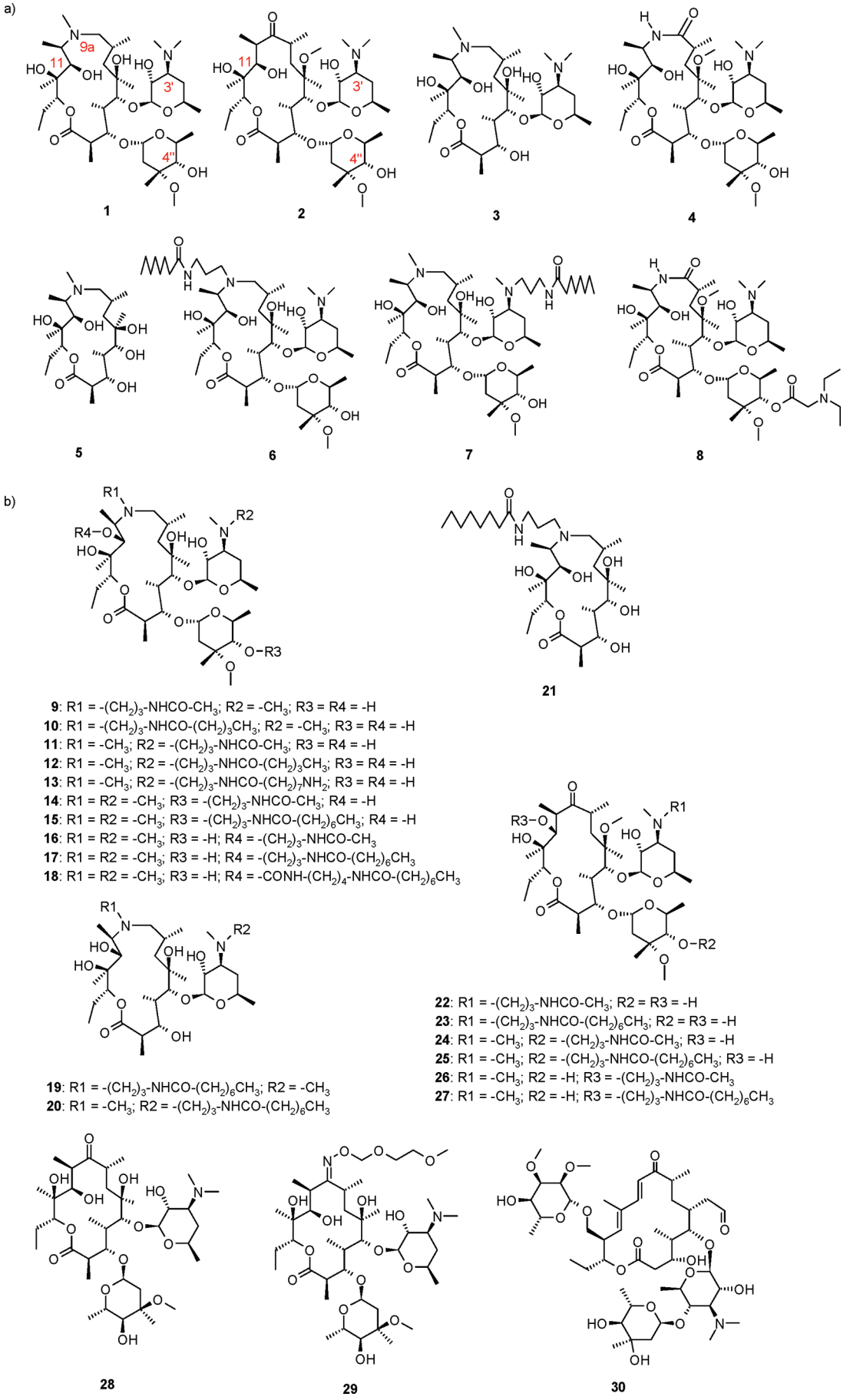


**Figure 1** (Continued on next page)

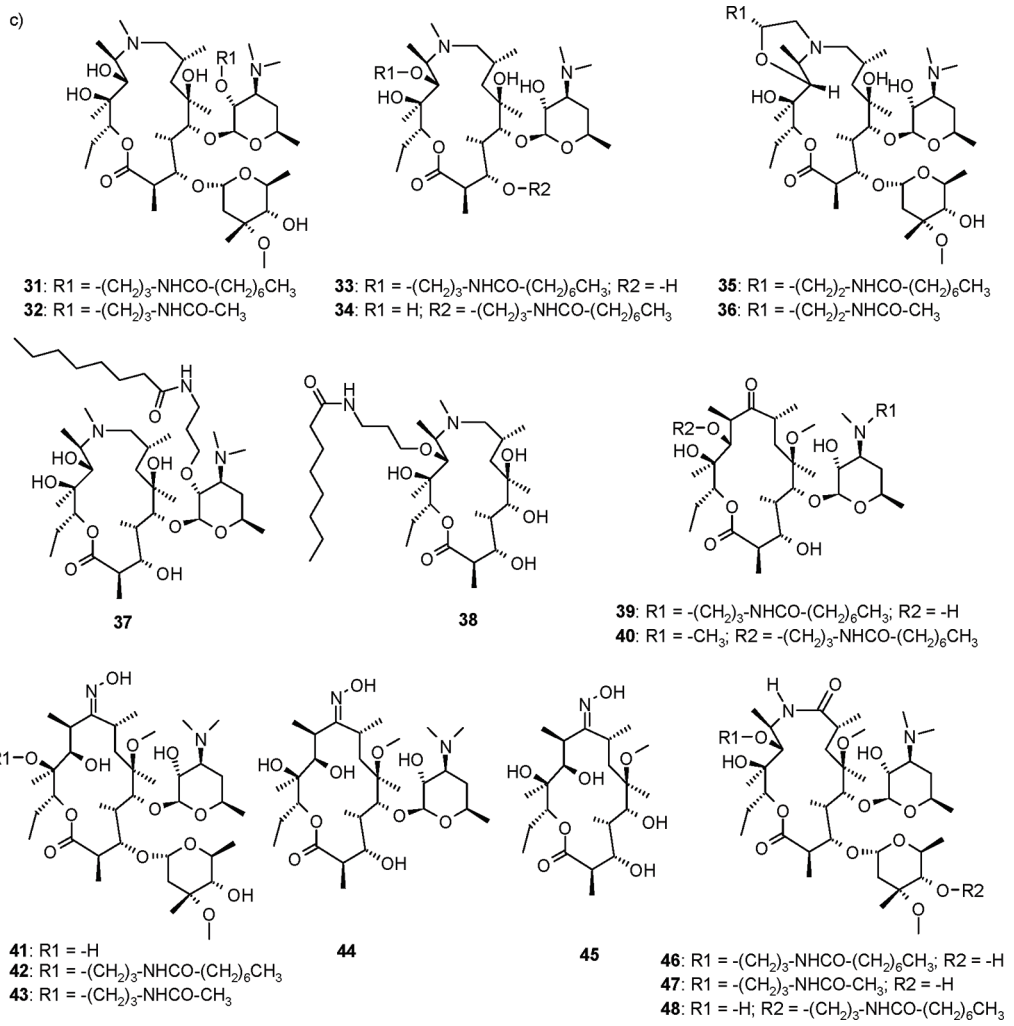


**Figure 1.** (a) Initial set of eight macolide compounds: **1**, azithromycin (9-deoxo-9a-aza-9a-methyl-9a-homoerythromycin A);[25] **2**, clarithromycin (6-*O*-methyl-erythromycin A);[26] **3**, descladinosyl azithromycin (5-*O*-desosaminyl-9-deoxo-9a-aza-9a-methyl-9a-homoerythronolide A);[25] **4**, 6-*O*-methyl 9a-lactam (6-*O*-methyl-9a-aza-9a-homoerythromycin A);[27] **5**, azithromycin aglycone (9-deoxo-9a-aza-9a-methyl-9a-homoerythronolide A);[25] **6**, 9a-*N*-demethyl-9a-[3-(octanoylamino)propyl]azithromycin (9-deoxo-9a-aza-9a-[3-(octanoylamino)propyl]-9a-homoerythromycin A) (see Experimental Section); **7**, 3′-*N*-demethyl-3′-*N*-[3-(octanoylamino)propyl]azithromycin (9-deoxo-9a-aza-9a-methyl-3′-*N*-demethyl-3′*N*-[3-(octanoylamino)propyl]-9a-homoerythromycin A) (see Experimental Section); **8**, 4″-*O*-(2-diethylaminoethanoyl)-6-*O*-methyl 9a-lactam (4″-*O*-(2-diethylaminoethanoyl)-6-*O*-methyl-9a-aza-9a-homoerythromycin A),[28] Positions used for substitution in compounds **1** and **2** are marked in red. (b) Rationally designed set of macrolide compounds used within the training set. (c) Rationally designed validation set.

relative to azithromycin's accumulation obtained in the same experiment. Retention in cells is expressed relative to the initially accumulated amount of a tested compound. Results are shown in Table 1.

Relative intensities of accumulation and retention for the considered set of macrolides correlate between most tested cell types, and they can be estimated quite well from results obtained on the NCI-H292 cell line (Table 2). Although differences in correlation coefficients were not statistically significant because of the small number of compounds, it is evident that most of the very mutually diverse cell types display high intercorrelations ($R > 0.90$) in cellular accumulation data (Table 2a). The largest deviations from the results of other cell types were observed for lung fibroblasts NHLF.

The best correlation of cellular accumulation data was found between the two cell types of similar epithelial morphology: lung carcinoma cell line NCI-H292 and primary culture of bronchial epithelial cells NHBE ($R = 0.99$).

Perhaps the most striking is the similarity of cellular accumulation results obtained in polymorphonuclear leukocytes (PMN) representing the phagocytic cell type and NCI-H292 lung epithelial cell line ($R = 0.98$). This correlation was further studied with 23 macrolides from the training set, and the result was confirmed ($R = 0.98$, with 95% confidence intervals 0.96, 0.99; data not shown). This result is even more interesting when taking into account the fact that in these two cell types the extracellular macrolide was removed in two different ways at the end of incubation: PMNs were washed through silicone oil, whereas NCI-H292 cells were washed with ice-cold PBS. Therefore, in this experimental setup, the amount of compound attached to the outer side of the cell, which should be completely removed only by centrifuging cells through silicone oil, was equally well removed by sequential washing in ice-cold PBS or can be neglected, since both washing procedures in two completely different cell types gave the same result.

Similarly, moderate to high correlations between most cell types studied were obtained for cellular retention data

**Table 1.** (a) Accumulation and (b) Retention of the Initial Eight Macrolides (Figure 1a) in the Seven Cell Types of Lung and Leukocytic Origin[a]

(a) Accumulation

| | PMN | | NHBE | | BSMC | | NHLF | | MDM | | TLy | | NCI-H292 | |
|---|---|---|---|---|---|---|---|---|---|---|---|---|---|---|
| compd | % azi | SD | % azi | SD | % azi | SD | % azi | SD | % azi | SD | % azi | SD | % azi | SD |
| **1** | 100 | | 100 | | 100 | 0 | 100 | | 100 | | 100 | | 100 | |
| **2** | 36 | 6 | 25 | 6 | 36 | 13 | 127 | 17 | 66 | 13 | 16 | 2 | 35 | 4 |
| **3** | 42 | 2 | 52 | 5 | 75 | 18 | 52 | 4 | 79 | 6 | 52 | 9 | 56 | 8 |
| **4** | 13 | 3 | 11 | 3 | 5 | 1 | 9 | 1 | 11 | 1 | 5 | 3 | 10 | 0 |
| **5** | 17 | 2 | 8 | 1 | 9 | 3 | 54 | 9 | 28 | 13 | 5 | 0 | 13 | 2 |
| **6** | 146 | 16 | 135 | 31 | 111 | 38 | 122 | 41 | 120 | 28 | 127 | 1 | 207 | 48 |
| **7** | 663 | 138 | 422 | 55 | 598 | 125 | 1699 | 60 | 1235 | 415 | 460 | 110 | 457 | 47 |
| **8** | 118 | 12 | 101 | 13 | 83 | 39 | 256 | 25 | 148 | 19 | 41 | 6 | 121 | 20 |

(b) Retention

| | PMN | | NHBE | | BSMC | | NHLF | | MDM | | TLy | | NCI-H292 | |
|---|---|---|---|---|---|---|---|---|---|---|---|---|---|---|
| compd | % ret | SD | % ret | SD | % ret | SD | % ret | SD | % ret | SD | % ret | SD | % ret | SD |
| **1** | 79 | 6 | 63 | 6 | 54 | 11 | 80 | 9 | 93 | 13 | 38 | 8 | 77 | 8 |
| **2** | 2 | 3 | 0 | 0 | 1 | 1 | 1 | 2 | 4 | 2 | 2 | 1 | 1 | 2 |
| **3** | 68 | 12 | 74 | 8 | 63 | 16 | 70 | 8 | 81 | 17 | 46 | 6 | 77 | 12 |
| **4** | 37 | 0 | 16 | 8 | 0 | 0 | 35 | 1 | 8 | 12 | 2 | 2 | 23 | 10 |
| **5** | 0 | 0 | 0 | 0 | 0 | 0 | 0 | 0 | 3 | 5 | 1 | 1 | 0 | 0 |
| **6** | 77 | 10 | 71 | 5 | 57 | 16 | 84 | 12 | 83 | 7 | 30 | 1 | 69 | 9 |
| **7** | 85 | 1 | 57 | 0 | 47 | 23 | 78 | 3 | 100 | 9 | 19 | 6 | 51 | 8 |
| **8** | 74 | 4 | 33 | 1 | 27 | 21 | 63 | 12 | 56 | 4 | 6 | 3 | 48 | 4 |

[a] To measure accumulation, cells were incubated with 3−20 $\mu$M macrolide for 3 h. To determine retention, drug-loaded cells were incubated in drug-free medium for 3 h. Intracellular concentration was determined by LC−MS/MS. Accumulation is expressed relative to azithromycin accumulation (100%) measured in the same experiment (% azi). Retention is expressed as a percentage of initially accumulated (% ret) compound that remained in cells after a 3 h washout.

**Table 2.** Cross-Correlation Coefficients with 0.95 Confidence Intervals (in Parentheses) for (a) Accumulation (ACC) and (b) Retention (RET) of the Initial Eight Macrolides (Figure 1a) within the Six Primary Cell Cultures and a Cell Line NCI-H292[a]

(a) ACC

| | NCI-H292 | PMN | NHLF | NHBE | TLy | MDM |
|---|---|---|---|---|---|---|
| PMN | 0.98 (0.89; 0.996) | | | | | |
| NHLF | 0.86 (0.395; 0.974) | 0.91 (0.573; 0.983) | | | | |
| NHBE | 0.99 (0.944; 0.998) | 0.98 (0.89; 0.996) | 0.82 (0.274; 0.966) | | | |
| TLy | 0.97 (0.839; 0.994) | 0.95 (0.743; 0.991) | 0.79 (0.193; 0.96) | 0.98 (0.89; 0.996) | | |
| MDM | 0.94 (0.698; 0.989) | 0.97 (0.839; 0.994) | 0.96 (0.79; 0.992) | 0.92 (0.613; 0.985) | 0.91 (0.573; 0.983) | |
| BSMC | 0.97 (0.839; 0.994) | 0.96 (0.79; 0.992) | 0.88 (0.462; 0.978) | 0.97 (0.839; 0.994) | 0.98 (0.89; 0.996) | 0.96 (0.79; 0.992) |

(b) RET[b]

| | NCI-H292 | PMN | NHLF | NHBE | TLy | MDM |
|---|---|---|---|---|---|---|
| PMN | 0.97 (0.839; 0.994) | | | | | |
| NHLF | 0.99 (0.944; 0.998) | 0.99 (0.944; 0.998) | | | | |
| NHBE | 0.99 (0.944; 0.998) | 0.95 (0.743; 0.991) | 0.98 (0.890;0.996) | | | |
| TLy | 0.85 (0.363; 0.972) | 0.74 (0.074; 0.949) | 0.79 (0.193; 0.96) | 0.90 (0.534; 0.981) | | |
| MDM | 0.95 (0.743; 0.991) | 0.90 (0.534; 0.981) | 0.94 (0.698; 0.989) | 0.97 (0.839; 0.994) | 0.91 (0.573; 0.983) | |
| BSMC | 0.93 (0.654; 0.987) | 0.89 (0.498; 0.980) | 0.90 (0.534; 0.981) | 0.95 (0.743; 0.991) | 0.93 (0.654; 0.987) | 0.96 (0.79; 0.992) |

[a] Prior to calculation all values were $\log_{10}$ transformed. [b] For the purpose of $\log_{10}$ transformation, zero values of retention were replaced with mean standard deviations.

(Table 2b). As T-lymphocytes have a very low amount of cytosol and lysosomes compared to other cell types, macrolides were least retained in them, and consequently, T-lymphocytes showed the trend of lowest correlation with other cell types based on retention data.

Moreover, similarity of accumulation and retention processes between different cell types has been confirmed by the multivariate principal component analysis (PCA) in terms of various physicochemical and structural descriptors (Supporting Information Figure S1).

Because of the similarity of the obtained results with other cell types, as well as the lower cost and easier handling, NCI-H292 cells were used in all further cellular PK experiments in order to build models for the predictions of cellular accumulation and retention of macrolides.

**Descriptive Analysis of Experimental Data.** Descriptive statistics of measured parameters are shown in Table 3. Experimental data for training (Figure 1a and Figure 1b) and validation (Figure 1c) compounds used in building and validation of models are available in Supporting Information Table S1. Differences between $\log P_{o/w}$ and $\log D_{o/w}$ reflect the amphiphilic nature of macrolides possessing both hydrophilic and lipophilic fragments. It is demonstrated by explicit values for these physicochemical parameters, as well as aqueous acid ionization constants.

Apart from two molecules without ionization centers, all other considered molecules carry at least one basic center.

**Table 3.** Descriptive Statistics for Experimentally Determined Accumulation and Retention in NCI-H292 Cells and Physicochemical Properties, Together with Molecular Weight and POS for Training (30 Compounds)/Validation (18 Compounds)/Extended Compound Set (85 Compounds)

| property | mean | median | min | max |
|---|---|---|---|---|
| NCI_H292 accumulation[a] | 134.8/267.8/319.4 | 45.7/134.8/79.9 | 0.8/0.4/0.4 | 755.6/1061.7/10073.5 |
| NCI_H292 retention[b] | 43.6/38.6/41.6 | 50.0/43.1/46.5 | 0/4.7/0 | 81.1/69.9/86.0 |
| log $P_{o/w}$ | 3.8/nd/nd | 3.6/nd/nd | 1.6/nd/nd | 6.3/nd/nd |
| log $D_{o/w}$ | 1.6/nd/nd | 1.7/nd/nd | −1.2/nd/nd | 3.8/nd/nd |
| p$K_{a,1}$ | 9.1/nd/nd | 9.1/nd/nd | 8.1/nd/nd | 10.4/nd/nd |
| p$K_{a,2}$ | 8.3/nd/nd | 8.4/nd/nd | 6.7/nd/nd | 9.1/nd/nd |
| ChromlogD | 3.3/4.5/4.1 | 3.1/4.6/3.7 | 1.2/2.3/1.2 | 6.4/6.7/9.9 |
| CHI IAM | 62.4/60.4/63.5 | 61.6/60.9/60.9 | 25.2/29.8/25.2 | 113.5/84.0/113.5 |
| PERM (nm/s) | 130.6/122/118 | 86/93/86 | 0/10/0 | 400/290/410 |
| solubility ($\mu$M) | 354/317/310 | 387/330.5/340.5 | 36/3/1 | 487/396/542 |
| POS | 1.6/1.3/1.6 | 2/1/2 | 1/0/0 | 3/2/3 |
| molecular weight[c] | 827.4/800.5/827.4 | 847.8/810.2/847.2 | 433.7/447.6/433.7 | 989.5/946.2/1256.8 |

[a] Cellular accumulation of a given compound is expressed as in Table 1. [b] Retention of a given compound is expressed as in Table 1. [c] For reference, molecular weights of clarithromycin and azithromycin are 748.1 and 749.1, respectively.

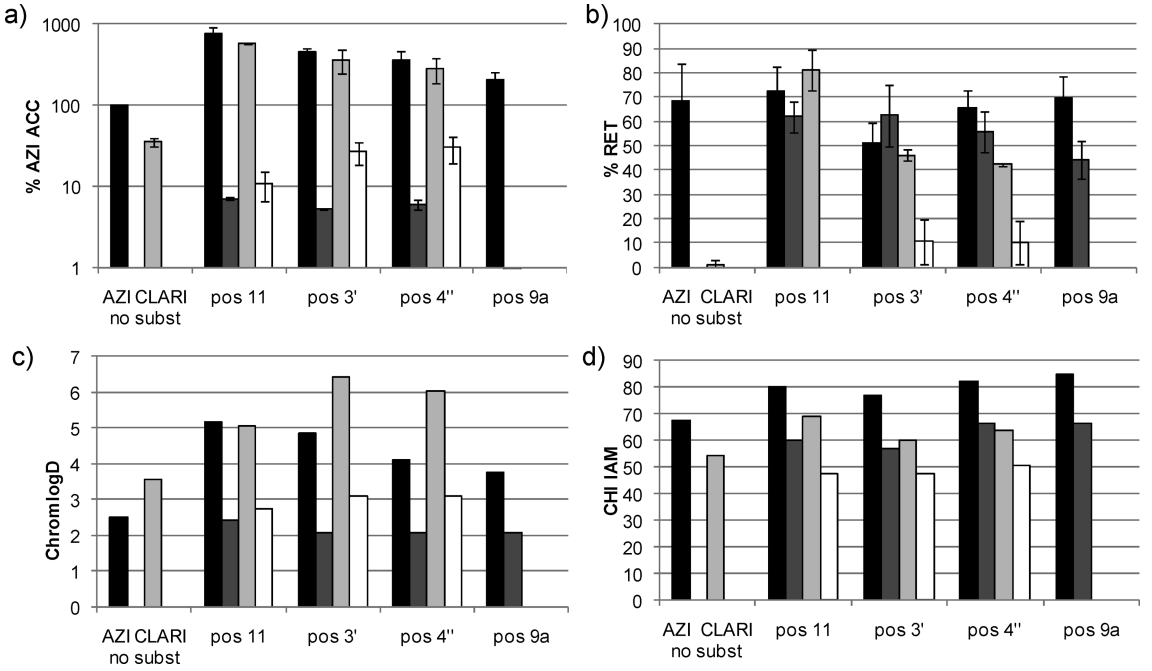


**Figure 2.** Effects of small structural changes on macrolide (a) accumulation and (b) retention in NCI-H292 cells, and physicochemical parameters (c) ChromlogD and (d) CHI IAM: black, azithromycin with 3-octanoylaminopropyl substituent; dark gray, azithromycin with 3-acetylaminopropyl; light gray, clarithromycin with 3-octanoylaminopropyl; white, clarithromycin with 3-acetylaminopropyl. Substitution positions in macrolide structures (denoted pos 11, 3′, 4″, and 9a) are depicted in Figure 1a (compounds **1** and **2**). The first two bars in each figure represent azithromycin and clarithromycin without substituents (no subst). For accumulation and retention, mean values of a minimum of three experiments are given and error bars represent SD. Data with structures are provided in Supporting Information Table S1. Accumulation and retention are expressed as in Table 1.

None of the compounds contain a negatively charged group. Values of acid/base ionization constants p$K_a$ indicate that the training set molecules are all positively charged at the physiological pH 7.4 and those molecules with two or three basic nitrogens carry a double or triple charge. The considered compounds are moderately soluble in water and moderately permeable through phospholipid membranes.

PCA and PLS analyses of all experimental and calculated parameters have been performed in order to identify molecular properties that affect the investigated biological processes (Supporting Information Figure S2). Molecular properties used in this study are experimentally determined physicochemical variables log $P_{o/w}$ and log $D_{o/w}$, chromatographically determined ChromlogD and CHI IAM, solubility (Sol), artificial membrane permeability (PERM), and acid−base equilibrium constants p$K_{a,i}$, pNF, and pCF_total and calculated structural descriptors hbd, hba, POS, hetrat, atom-based E-state descriptors,[29] and Abraham descriptors.[30−32] All descriptors are described in Experimental Section. Accumulation in NCI-H292 was found to be proportional to lipophilicity parameters log $D_{o/w}$ and ChromlogD. Retention within cells was found to be related to positive charge (POS), amount of charged species (pCF_total), and affinity for phospholipids (CHI IAM).

Effects of small structural changes on cellular pharmacokinetics can be extracted from measured data for rationally designed compounds with respect to macrolide scaffolds, substitution sites, and type of substituent. In Figure 2 azithromycin and clarithromycin derivatives substituted by

3-octanoylaminopropyl (long chain) and 3-acetylaminopropyl (short chain) on 3′, 4″, 11, and 9a positions (Figure 1a) are compared regarding their lipophilicity (ChromlogD), binding to phospholipids (CHI IAM), and accumulation and retention in NCI-H292 cells.

Substitutions of both scaffolds with long chain at all four positions resulted in significant increases in lipophilicity and accumulation. Substitutions with less lipophilic (short) linker drastically decreased accumulation of azithromycin compounds, without significant changes in lipophilicity. Interestingly, short linker did not have such a pronounced effect on accumulation of clarithromycin derivatives, in agreement with trends in ChromlogD. Since the effect of a short linker on azithromycin scaffold cannot be rationalized through the drop in lipophilicity, further studies taking into account the effect of 3D structure are ongoing. Effect of the 3D structure is further evidenced by the differences in cellular accumulation with respect to the substitution position, which indicates nonadditive effect of structural moieties in macrolide structure. For example, spatially close 11 and 9a positions have the largest differences in cellular accumulation (756% vs 207% of azithromycin value for azithromycin compounds substituted with long linker).

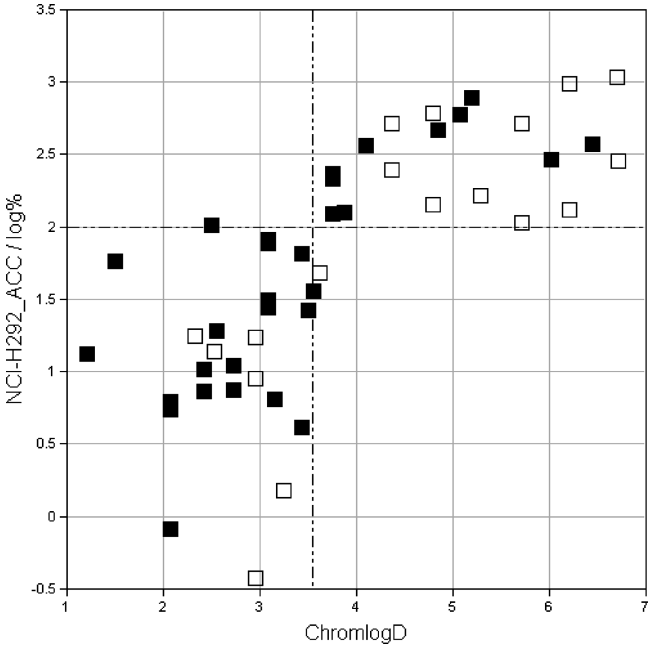


**Figure 3.** First model ((1), Table 4) for cellular accumulation (NCI-H292_ACC) of macrolides in NCI-H292 cells based only on chromatographically determined lipophilicity parameter ChromlogD. Accumulation is expressed as log % of azithromycin accumulation. Training set is represented by closed symbols. Validation set is represented by open symbols.

Regardless of the intensity of accumulation and substitution position, azithromycin derivatives substituted with both types of linker retained azithromycin's high retention in cells, whereas among compounds with clarithromycin scaffold only derivatives with the long linker were well retained (Figure 2b). Similar to retention results, among compared compounds, clarithromycin scaffold alone and clarithromycin substituted with the short linker displayed the lowest binding to phospholipids (CHI IAM, Figure 2d).

**Models for Cellular Accumulation.** Simple two-class models (Table 4) for cellular accumulation were obtained by decision tree approach. Compounds with accumulation greater than that of azithromycin, i.e., 100%, were considered as highly accumulated, and otherwise they were low accumulated. Accordingly, in the training/validation set there were 10/11 highly and 20/7 low accumulated compounds.

Chromatographically determined lipophilicity was the most important root parameter for description of accumulation within NCI-H292 cells. All compounds from the training set were correctly classified based on ChromlogD only, and high prediction power of the model (1) was confirmed by correct classification of 94.4% of validation set compounds (Figure 3). Stability of the model was tested by merging training and validation sets (model (2)), and again ChromlogD alone was sufficient to correctly classify all of the compounds. Two of the validation set compounds that were misspredicted by the first model (1) were correctly classified in the new model because of the obtained slight increase in the cutoff value.

Bearing in mind that the described models were developed on the structurally analogous compounds (Figure 1) to expand the diversity of the rationally designed training and validation sets, 37 new macrolides synthesized within a drug discovery research program on novel anti-inflammatory macrolides were added to analysis. The ChromlogD model ((2), Table 4) correctly predicted 81.1% of 37 novel macrolides showing general applicability of the model. By the fusing of all training, validation, and proprietary anti-inflammatory compounds together in the extended set of 85 compounds, a very good model (3) was still obtained with ChromlogD only. In addition, two improved and mutually equivalent models (4 and 5) were further developed. They recognize CHI IAM or POS as additional important variables accounting for contributions of a compound's basicity to the cellular accumulation (96.5% total success) (Figure 4).

**Table 4.** Statistical Parameters[a] for the Two-Class Decision Tree Models for the Accumulation within NCI-H292 Cells[b]

| (model no.) descriptor (cutoff) | *N* | total success, % | sensitivity, % | specificity, % | κ |
|---|---|---|---|---|---|
| Training/Validation | | | | | |
| (1) ChromlogD (≤3.55, low ACC) | 30/18 | 100.0/94.4 | 100.0/100.0 | 100.0/85.7 | 1.00/0.88 |
| Training + Validation | | | | | |
| (2) ChromlogD (≤3.61, low ACC) | 48 | 100.0 | 100.0 | 100.0 | 1.00 |
| Extended Set | | | | | |
| (3) ChromlogD (≤3.61, low ACC) | 85 | 91.8 | 97.5 | 86.7 | 0.84 |
| (4) ChromlogD and CHI IAM (Figure 5a) | 85 | 96.5 | 95.0 | 97.8 | 0.93 |
| (5) ChromlogD and POS (Figure 5b) | 85 | 96.5 | 95.0 | 97.8 | 0.93 |

[a] *N* is a number of compounds used for model building, while other parameters are described in the Experimental Section. [b] In all models, compounds accumulated with ≤Azi (100%) are defined as low accumulated and otherwise as highly accumulated. Descriptor cutoff values are given in parentheses.

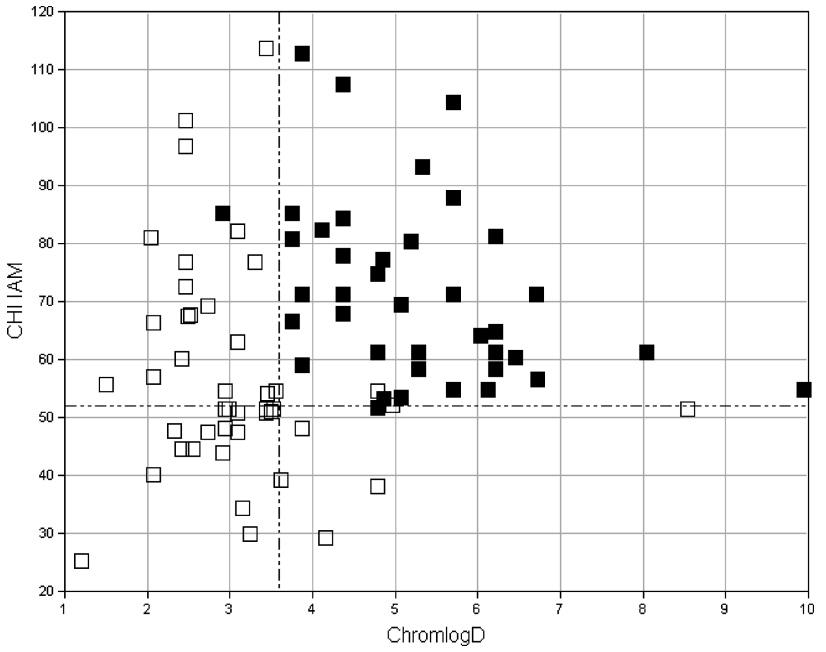


**Figure 4.** Dependence of cellular accumulation on ChromlogD and CHI IAM for the extended set of 85 compounds. Closed symbols represent accumulation of > 100%, that is, > Azi. Open symbols: represent accumulation ≤ 100%, that is, ≤ Azi.

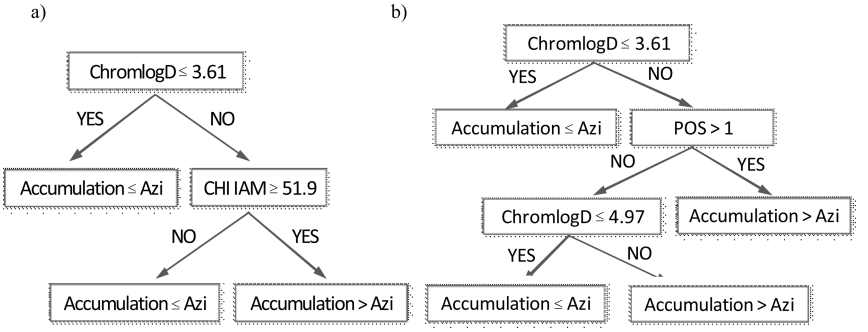


**Figure 5.** Hierarchical decision trees for accumulation within the NCI-H292 cells for the extended set (Table 4): (a) model 4 based on ChromlogD and CHI IAM; (b) model 5 based on ChromlogD and POS.

Developed decision tree models are graphically presented in Figure 5. Although CHI IAM variable contains more information regarding compound affinity for phospholipids, simple POS variable could be used instead when CHI IAM data are not available.

It is interesting to observe that models developed for a rationally designed set adequately describe the dependence of accumulation upon ChromlogD, which reflects positive contribution of lipophilicity to passive permeability of macrolides through cellular membranes. However, good passive permeability may not be enough for a compound to be accumulated within the cell. It should be either retained within or actively pumped into the cell. In order to be retained, a compound could be bound mostly nonspecifically to proteins and phospholipids. It has been shown that high IAM binding relative to the albumin binding correlates with high volume of distribution of known drugs[33] which is proportional to compound's distribution between the tissue and plasma compartment. It was also shown that positively charged compounds bind strongly with the negatively charged phospholipids within the cell. These findings are in agreement with models developed for the more diverse extended set.

Further valuable outcomes of the developed models are specifically determined cutoff values, which may be used for future design of new macrolide compounds and optimization of their cellular accumulation. Important for macrolides, the most significant parameters are chromatographically measured in high-throughput mode, which enables screening of a large number of compounds in small amounts.

Apart from passive transport, macrolides were reported to interact with several organic anion transporters albeit mainly as noncompetitive inhibitors rather than substrates.[34] However, it is less likely that our results are significantly influenced by active transport, since in the seven tested, diverse cell types relative estimations of accumulations highly correlate. In the case of active transport the same putative transporter should be present in at least five tested cell types for which the results highly correlate (Table 2a). Where weaker correlation with other cell types was observed (e.g., NHLF), we may speculate that a transporter specific for these cell types may be responsible for the decline from the results obtained on other cells.

Dependence of cellular accumulation on different lipophilicity measures, ChromlogD, log $D_{o/w}$, and log $P_{o/w}$ was also analyzed, and two-class models were developed (Table 5).

The NCI-H292 accumulation correlates with both log $D_{o/w}$ and ChromlogD ($R^2$ of 0.63 and 0.55, respectively), while correlation with log $P$ is rather low ($R^2 = 0.27$). However, with log $D_{o/w}$ no unique cutoff value was obtained. Better class differentiation was achieved with ChromlogD most likely because this chromatographically determined lipophilicity more closely mimics molecular interactions with the alkyl chains of the membranes while log $D_{o/w}$ describes the distribution between two unordered phases. These findings are also reflected in quite low correlation between ChromlogD and log $D_{o/w}$ ($R^2$ of 0.39) for 29 of the training macrolides. Additional practical advantage of ChromlogD over log $D_{o/w}$ is evident in a much smaller quantity of compound needed and high throughput of the measurement.

Besides decision tree models, continuous PLS analysis for NCI-H292 cellular accumulation was also performed using the whole set of parameters. Analogous to classification models, the PLS models developed in terms of various combinations of descriptors revealed that the predictive and stable models always contain at least one lipophilicity related parameter such as ChromlogD, log$D_{o/w}$, or calculated E-state structural variable corresponding to lipophilic alkyl chains. Other structural motifs as represented by atom-based E-state descriptors or other molecular features were not found to be important for the description of macrolide accumulation within NCI-H292 cells, confirming again that accumulation is to large extent a function of a whole molecular property, lipophilicity. However, accuracy of the PLS models was slightly lower than that of more simple and straightforward classification models.

**Models for Cellular Retention.** The first two-class model for cellular retention of macrolides in NCI-H292 cells obtained with the training set was based only on CHI IAM (Table 6, Figure 6). Compounds with retention of $<30\%$ were considered to have low retention, and those with values of $\geq 30\%$ have high retention. Accordingly, in the training/validation set there were 9/7 low and 20/9 highly retained compounds within the NCI-H292 cells. For two compounds in training set and two in the validation set retention could not be accurately determined because of the extremely low accumulation and weaker response of the MS detector.

According to the decision tree approach (Table 6), for macrolide retention CHI IAM and POS are comparably differentiating descriptors giving models 1, 2, 4, and 5 with comparable statistical quality. For the considered macrolides, the CHI IAM values increase significantly with increasing positive charge (one-way paired $t$ test with $p < 3.8 \times 10^{-49}$), which is in accordance with the known influence of positive charge on phospholipid binding.[33] A two-variable model (3) including POS and ChromlogD was also developed. However, its predictive power for validation compounds is lower compared with the POS model (2).

By the merging of training and validation sets, the same root variables were obtained, POS and CHI IAM. However,

**Table 5.** Cutoff Values Defined in Terms of ChromlogD, log $D_{o/w}$, and log $P_{o/w}$ for Differentiation between High and Low Accumulated Training Set Compounds within NCI-H292 Cells

| descriptor | decision tree cutoff | N | total success, % |
|---|---|---|---|
| ChromlogD | 3.55 | 30 | 100.0 |
| log $D_{o/w}$ | complex hierarchical tree, no unique cutoff | 29 | 96.7 |
| log $P_{o/w}$ | 5.15 | 29 | 83.3 |

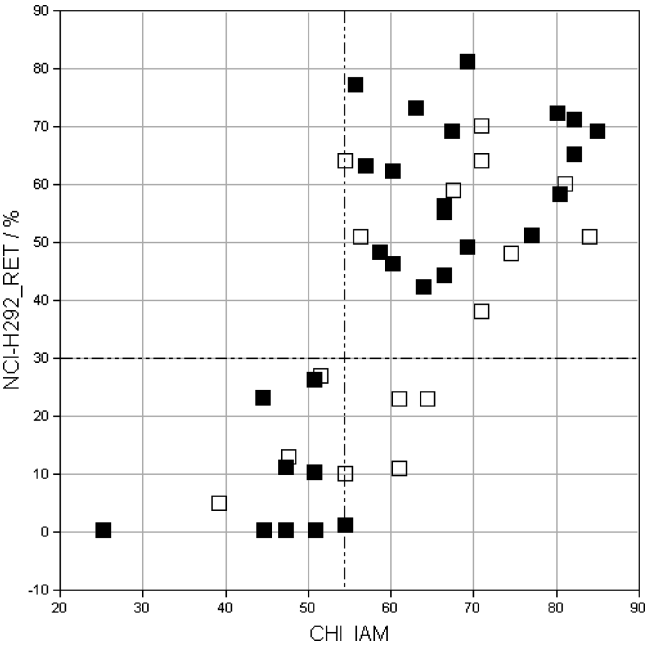


**Figure 6.** First model ((1), Table 6) for cellular retention (NCI-H292_RET) of macrolides in NCI-H292 cells based only on CHI IAM, developed with the training set (closed symbols) and tested with the validation set (open symbols).

**Table 6.** Statistical Parameters[a] for the Two-Class Models for the Retention within NCI-H292 Cells[b]

| (model no.) descriptors (cutoffs) | $N$ | total success, % | sensitivity, % | specificity, % | $\kappa$ |
|---|---|---|---|---|---|
| Training/Validation | | | | | |
| (1) CHI IAM ($\leq$54.4, low RET) | 28/16 | 100.0/75.0 | 100.0/88.9 | 100.0/57.1 | 1.00/0.48 |
| (2) POS ($\leq$1, low RET) | 28/16 | 89.3/87.5 | 84.2/77.8 | 100.0/100.0 | 0.77/0.75 |
| (3) POS and ChromlogD (POS $\leq$ 1 and ChromlogD $\leq$ 4.1, low RET) | 28/16 | 100.0/75.0 | 100.0/100.0 | 100.0/57.1 | 1.00/0.46 |
| Training + Validation | | | | | |
| (4) CHI IAM ($\leq$51.4, low RET) | 44 | 90.9 | 81.3 | 96.4 | 0.80 |
| (5) POS ($\leq$1, low RET) | 44 | 88.6 | 82.1 | 100.0 | 0.77 |
| (6) POS and CHI IAM (Figure 7a) | 44 | 93.2 | 100.0 | 81.3 | 0.85 |
| (7) POS and ChromlogD (Figure 7b) | 44 | 93.2 | 100.0 | 81.3 | 0.85 |
| Extended Set | | | | | |
| (8) POS and CHI IAM (Figure 7a) | 80 | 92.5 | 96.2 | 85.2 | 0.83 |
| (9) POS and ChromlogD (Figure 7b) | 80 | 92.5 | 98.1 | 81.5 | 0.83 |

[a] All statistical parameters are defined as in Table 4. [b] In all models compounds retained within the NCI-H292 cells at 30% and more are considered highly retained. Otherwise, compounds are poorly retained. Descriptor cutoff values are given in parentheses.

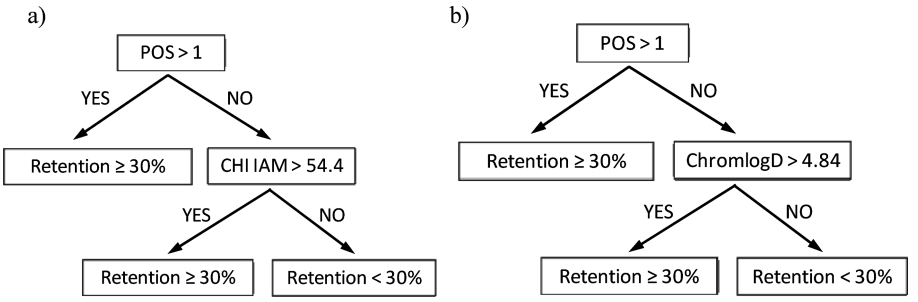


**Figure 7.** Hierarchical decision trees for retention of macrolides within the NCI-H292 cells developed with the training and validation sets combined and confirmed with the extended set (Table 6): (a) models 6 and 8 based on POS and CHI IAM; (b) models 7 and 9 based on POS and ChromlogD. Cutoff for ChromlogD in model 9 is 4.97.

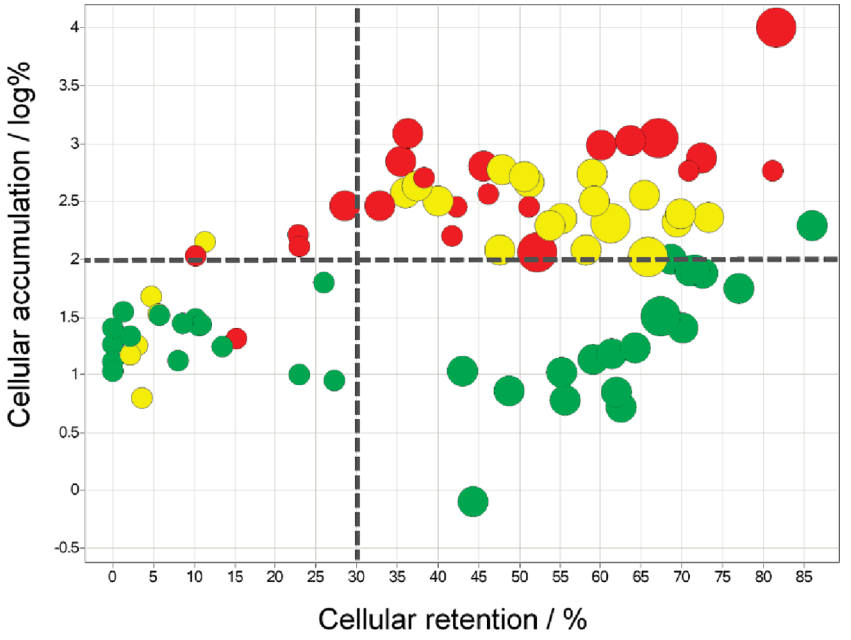


**Figure 8.** Relationship between cellular accumulation and cellular retention in NCI-H292 cells, POS, and ChromlogD for all studied compounds (extended set). Compounds are colored according to ChromlogD: green, < 3.61; yellow, 3.61−4.84; red, >4.84. Symbol size is according to the number of positively charged centers (POS): big, POS = 3 (6 compounds); medium, POS = 2 (41 compounds); small, POS = 1 (31 compounds).

additional two-variable models combining POS with CHI IAM (model 6) (Figure 7a) or ChromlogD (model 7) (Figure 7b) resulted in improved accuracy (Table 6), indicating the contribution of lipophilicity to cellular retention. Models obtained with merged training and validation sets were further justified by using 35 diverse anti-inflammatory macrolides with total success ($\kappa$ value) of 85.3 (0.70), 91.4 (0.81), 94.1 (0.87), 97.1 (0.93) for models 4, 5, 6, 7 (Table 6), respectively.

Analogous results with the same variables and their cutoff values were obtained with the extended set as well (Table 6), confirming stability of the developed retention models. Such consistence of the accumulation and retention models reveals that the key physicochemical parameters for the examined biological processes were determined resulting in not only statistical but also mechanistic models. Since the same variables were found to be important for describing both processes, this result supports contribution of retention to macrolide accumulation within cells, as quantified by the retention branch (Figure 7b) within the decision tree for accumulation (Figure 5b).

In addition to classification, continuous PLS models were also developed. However, the PLS analyses in terms of the all used molecular descriptors did not reveal additional molecular parameters that significantly influence macrolide cellular retention apart from POS, CHI IAM, and Chromlog, which is analogous to the classification models.

Interestingly, the chromatographic peaks of most of the macrolides were quite wide on the IAM PC DD stationary phase, suggesting slow kinetics for the phospholipid binding of the macrolides. While the chromatographic retention time is proportional to the distribution coefficient of the compounds between aqueous buffer and immobilized artificial membrane, the peak width might provide information about the speed of the partitioning process.[35] The observed slow kinetics of the phospholipid partitioning of the compounds might mimic the observed long cellular retention of the macrolides relative to the small molecules.

**Compound Properties Affecting Cellular Accumulation and Retention of Macrolides.** In the present study both cellular accumulation and retention of macrolides were shown to be predictable from the chromatographically determined lipophilicity ChromlogD and the number of positively charged centers (POS) (see Figure 5b and Figure 7b). In Figure 8 the overall relationship between these four parameters is presented.

Macrolides with more than one positively charged center (basic nitrogen atom with $pK_{a,i}$ of around 8) are all well retained in cells, and they accumulate more than azithromycin if their ChromlogD value is higher than or equal to 3.61 (upper right quadrant). Otherwise they have lower accumulation than azithromycin (lower right quadrant). On the other hand, if a macrolide has one positively charged center, it will be low retained and accumulated less than azithromycin (lower left quadrant), unless they are very lipophilic (ChromlogD > 4.84), which makes them highly accumulated (> azi) and highly retained (upper right quadrant). Among compounds considered in this study there were only five compounds that accumulated more than azithromycin but were low retained (upper left quadrant). As such, they were misclassified by this model, although they were very close to the cutoff values. This analysis gives a simple and quantitative way to classify macrolide compounds according to their cellular PK properties.

Macrolides have been shown by several groups to accumulate within cells because of their sequestration in lysosomes.[15] The two main factors causing lysosomal accumulation of basic compounds have been proposed: pH partitioning resulting in cationic entrapment of weak bases in acidic compartments, and drug lipophilicity resulting in drug binding to acidic lipids in the lysosomal membrane.[36,37] Our results support both of these schemes.

Recently, Trapp et al.[38] reported calculated cell model for estimating accumulation of molecules in lysosomes, as well as for defining the impact of compound's ability to increase lysosomal pH and by that limit its own accumulation. The model is based on passive diffusion and is defined in terms of dissociation constants ($pK_a$), charge, and lipophilicity ($\log K_{ow}$ ($\log P_{o/w}$)). Our results are in accordance with their findings. For example, the model by Trapp et al.[38] predicts that accumulation in lysosomes is optimal for bases with $pK_a \approx 8$. At least one of the $pK_a$ constants in considered macrolides is close to 8 (Table 3 and Supporting Information Table S1). However, since 14- and 15-membered macrolides used in this study do not differ significantly in their $pK_a$ values, the number of positively charged centers (POS) alone is sufficient for characterizing amine properties of these molecules contributing to cellular accumulation and retention. In addition to cationic trapping at lysosomal pH $\approx$ 5, an increase in lipophilicity of basic drugs increases the concentration within lysosomes probably because of interaction with the lipids of the lysosomal membrane.[36,38,39] Reported observations are in agreement with the models obtained in our study. However, we found a chromatographically determined parameter ChromlogD as the best lipophilicity descriptor of macrolide cellular accumulation compared with $\log P_{o/w}$ and $\log D_{o/w}$ (Table 5 and Supporting Information Table S1).

The ability of a drug to accumulate in lysosomes has a significant impact on its half-life in plasma and tissues,[40] as well as on its tissue distribution in vivo, enabling it to reach much higher concentrations in lysosome-rich tissues like lungs, liver, or kidney, compared to muscle or heart.[41,42] Lipophilicity was also shown to play a significant role in tissue distribution, where a correlation between octanol–water partitioning coefficient of various drugs and tissue-plasma concentration ratio was reported.[36] The strongest impact of lipophilicity on volume of distribution ($V_{dss}$) was reported for basic drugs, whereas the effect is less pronounced for neutral, acidic, and zwitterionic drugs.[19] Because in our study the same findings were obtained for macrolide cellular accumulation, they seem to behave in a similar fashion as small molecules.

Even though the mentioned reports, either of in vitro cellular or lysosomal accumulation or of in vivo tissue distribution, recognize the importance of lipophilicity, positive charge, and binding to phospholipids, their quantitative criteria were not directly transferable to macrolides. In the present study we have shown how these molecular characteristics, determined by high-throughput chromatographic measurements, with clear quantitative cutoffs affect the extent of cellular accumulation and retention of compounds of macrolide class.

## Conclusion

Extensive cellular accumulation and retention studies in different cell types and physicochemical profiling of macrolides have been performed. Collected results were analyzed in the broader context of known properties describing cellular PK phenomena for small molecules.

The NCI-H292 cell line was determined as a representative cellular model for estimation of cellular accumulation and retention of macrolides in several very diverse primary cell types.

Discrimination between macrolides with high or poor accumulation and retention within cells was achieved by only two physicochemical parameters ChromlogD and CHI IAM, chromatographically determined by HTS approach. For considered, basic macrolide compounds, the CHI IAM parameter can be replaced by a simple number of positively charged atoms within a molecule (POS). The simple decision tree models for the accumulation and retention within the NCI-H292 were built in terms of these three parameters.

For both considered biological processes, the obtained models are two-class with cutoff values of 100% for the cellular accumulation and 30% for the retention. In the case of the cellular accumulation, the root variable is the hydrophobicity parameter ChromlogD while CHI IAM or POS contributes to additional fine-tuning. In contrast, for the cellular retention, the root variable is POS while ChromlogD or CHI IAM contributes to fine-tuning. In other words, the critical molecular property for cellular accumulation of a basic macrolide is lipophilicity, while for retention it is a charge.

Our results support observations that macrolides accumulate within cells because of their sequestration in lysosomes, which is determined mostly by their lipophilicity and cationic nature at the physiological pH. Similarly, experimentally determined accumulation data of tested macrolides in most of the tested cell types support passive diffusion, rather than active transport, as a dominant driving force for macrolide cellular accumulation.

Compared with models determined in terms of only calculated structural descriptors, the employed property-based approach is structurally more robust, provided that the compounds considered have the same mechanism of accumulation and retention.

The developed models have been used for classifying and ranking newly synthesized anti-inflammatory macrolides. Depending on the intended indication, presented results may help in the design of macrolide compounds within the desirable range of cellular accumulation and retention in order to fine-tune their in vivo PK properties.

## Experimental Section

**Compound Synthesis. General Methods.** All glassware was oven-dried before used in connection with an inert atmosphere. Concentrations were performed under reduced pressure at < 40 °C (bath temperature). Thin layer chromatography was performed using Merck silica gel 60 F-254 plates using DCM/MeOH/$NH_4OH$ (aq, 25%) = 60:10:1 (by volume) as mobile phase with detection by UV, then charring with 5% $H_2SO_4$ in EtOH. Column chromatography was performed on Supelco (5 g, 20 g) and Isolute (10 g) flash silica prepacked columns (0.035−0.070 mm) preconditioned with DCM, using DCM/MeOH/$NH_4OH$ (aq, 25%) = 97:2:0.5 (by volume) as mobile phase. Room temperature was 23 °C. NMR spectra were recorded at room temperature on a Bruker (500 MHz) instrument. Chemical shifts are reported in ppm ($\delta$) relative to $Me_4Si$ as an internal standard. Unless otherwise stated, all materials were obtained from commercial suppliers and used without further purification. DCM was dried over 4 Å molecular sieves before use. The purity of final compounds was assessed by analytical LC−MS method and found to be ≥95% unless otherwise stated. The LC−MS analyses were performed using Waters Acquity UPLC instrument equipped with diode array detector and MS detector, Waters SQD, using the following parameters: column, Waters Acquity UPLC BEH C18, 2.1 mm × 50 mm, 1.7 $\mu$m particles; mobile phase A, 0.1% HCOOH in water; mobile phase B, 0.1% HCOOH in MeCN; isocratic 5% B in 1.5 min, then gradient 5−80% B in 7.25 min followed by 1.25 min at 90% B.

**Synthetic Procedures. General Microwave Assisted Amidation Procedure.** PS-CDI (1.3 equiv) was added into a dry reaction vessel. A solution of octanoic acid (1 equiv) and HOBt (0.7 equiv) in a mixture of $CH_2Cl_2$ (1 mL) and DMF (0.15 mL) prepared in a separate vial was added onto a dry resin followed by additional 1 mL of $CH_2Cl_2$ (from washing the vial). The mixture was stirred at room temperature for 5 min, upon which the corresponding macrolide amine 9-deoxo-9a-aza-9a-demethyl-9a-(3-aminopropyl)-9a-homoerythromycin A[43] (1 equiv), dissolved in 1 mL of $CH_2Cl_2$, was added followed by additional 1 mL of $CH_2Cl_2$ (from washing the vial). The reaction mixture was heated in a microwave oven (Initiator EXP, Biotage) at 70 °C for 5−10 min. After completion of the reaction HOBt was scavenged using PS-TRISAMINE (5 equiv) for 2−6 h at room temperature. Product was separated from the resin by filtration and the resin additionally washed with DCM (4 × 1 mL). Resulting filtrate was concentrated under reduced pressure. Crude residues were combined together and purified by column chromatography [DCM/(MeOH/$NH_4OH$ = 9:1.5) = 100:0 → 94:6].

**9-Deoxo-9a-aza-9a-demethyl-9a-[(3-octanoylamino)propyl]-9a-homoreythromycin A (6).** $^1$H NMR (500 MHz, DMSO-$d_6$) [$\delta$/ppm]: 7.74 (t, 1 H, $J$ = 5.5 Hz), 4.88 (dd, 1 H, $J$ = 10.2, 2.3 Hz), 4.79 (d, 1 H, $J$ = 4.9 Hz), 4.41 (d, 1H, $J$ = 7.3 Hz), 4.29 (s, 1 H), 4.24 (d, 1 H, $J$ = 7.3 Hz), 4.06 (m, 1 H), 4.00 (br s, 2 H), 3.95 (d, 1 H, $J$ = 6.7 Hz), 3.66 (m, 1 H), 3.50 (m, 2 H), 3.22 (s, 3 H), 3.03 (m, 1 H), 2.97 (dt, 2 H, $J$ = 12.4, 6.3 Hz), 2.90 (dd, 1 H, $J$ = 8.8, 7.3 Hz), 2.78 (br s, 1 H), 2.70 (m, 2 H), 2.53 (dd, 1 H, $J$ = 11.0, 3.0 Hz), 2.43 (m, 2 H), 2.26 (d, 1 H, $J$ = 15.0 Hz), 2.21 (s, 6 H), 2.06 (dd, 1 H, $J$ = 13.0, 11.0 Hz), 2.01 (t, 2 H, $J$ = 7.6 Hz), 1.94 (m, 1 H), 1.89 (m, 1 H), 1.76 (m, 1 H), 1.63 (m, 1 H), 1.58 (m, 1 H), 1.48 (m, 5 H), 1.37 (m, 2H), 1.26 (m, 2 H), 1.23 (br s, 4 H), 1.19 (s, 3 H), 1.15 (d, 3 H, $J$ = 6.1 Hz), 1.13 (s, 3 H), 1.09 (d, 3 H, $J$ = 7.3 Hz), 1.06 (d, 3 H, $J$ = 6.1 Hz), 1.05 (m, 1 H), 0.98 (m, 9 H), 0.85 (m, 6 H), 0.79 (t, 3 H, $J$ = 7.3 Hz); $^{13}$C NMR (126 MHz, DMSO-$d_6$) [$\delta$/ppm]: 176.64 (s), 172.14 (s), 102.29 (s), 95.16 (s), 82.79 (s), 78.08 (s), 77.61 (s), 76.62 (s), 75.16 (s), 74.58 (s), 73.70 (s), 72.99 (s), 70.93 (s), 67.28 (s), 65.08 (s), 64.84 (s), 63.14 (s), 60.24 (s), 49.06 (s), 48.61 (s), 44.47 (s), 40.62 (s), 37.19 (s), 35.73 (s), 35.04 (s), 31.44 (s), 30.36 (s), 28.85 (s), 28.15 (s), 27.60 (s), 27.31 (s), 25.63 (s), 22.63 (s), 22.33 (s), 21.68 (s), 21.57 (s), 21.24 (s), 18.73 (s), 18.40 (s), 15.19 (s), 14.19 (s), 11.24 (s), 9.61 (s). MS (ESI) $m/z$: 918.0 (calcd $[M + H]^+$ 918.0), purity 98.5%.

**General Classical Amidation Procedure.** Octanoic acid (1.1 equiv) was dissolved in THF (15 mL). The solution was cooled to 0 °C. $Et_3N$ was added (10.0 equiv), followed by HOBt (2 equiv), the corresponding macrolide amine, 9-deoxo-9a-aza-9a-methyl-3′-*N*-demethyl-3′-*N*-(3-aminopropyl)-9a-homoerythromycin A,[44] and EDC·HCl (4 equiv). The reaction mixture was stirred under an inert atmosphere (argon), allowing it to gradually reach room temperature. Stirring was continued until complete consumption of starting material, typically 4−18 h. The precipitate was filtered off and the filtrate concentrated under reduced pressure. The residue was dissolved in DCM (20 mL), washed with saturated $NaHCO_3$ (3 × 15 mL) and brine (3 × 15 mL), and dried over anhydrous $Na_2SO_4$. The solvent was removed under vacuum, and the residue was purified by column chromatography (DCM/MeOH/$NH_4OH$ = 100/2/0.1 → 100/2/0.2 → 100/2/0.5).

**9-Deoxo-9a-aza-9a-methyl-3′-*N*-demethyl-3′*N*-[3-(octanoylamino)propyl]-9a-homoerythromycin A (7).** $^1$H NMR (500 MHz, $CDCl_3$) [$\delta$/ppm]: 6.70 (t, 1 H, $J$ = 5.2 Hz), 5.14 (d, 1 H, $J$ = 4.9 Hz), 4.97 (br s, 1 H), 4.70 (dd, 1 H, $J$ = 10.1, 2.4 Hz), 4.43 (d, 1 H, $J$ = 7.3 Hz), 4.27 (dd, 1 H, $J$ = 4.0, 1.8 Hz), 4.08 (dq, 1 H, $J$ = 9.8, 6.1 Hz), 3.68 (s, 1 H), 3.65 (d, 1H, $J$ = 7.3 Hz), 3.51 (m, 1 H, $J$ = 10.7, 6.1, 6.1, 6.1, 1.2 Hz), 3.33 (s, 3 H), 3.31 (m, 3 H), 3.05 (t, 1 H, $J$ = 9.5 Hz), 2.98 (br.s., 1 H), 2.75 (dq, 1 H, $J$ = 7.3, 4.6 Hz), 2.70 (q, 1 H, $J$ = 7.0 Hz), 2.64 (dd, 1 H, $J$ = 13.1, 6.7 Hz), 2.55 (d, 1 H, $J$ = 10.4 Hz), 2.57 (m, 1 H), 2.45 (dt, 1 H, $J$ = 12.4, 6.1 Hz), 2.35 (d, 1 H, $J$ = 15.3 Hz), 2.33 (s, 3 H), 2.26 (s, 3 H), 2.22 (d, 1 H, $J$ = 10.1 Hz), 2.13 (t, 2 H, $J$ = 7.9 Hz), 2.06 (t, 1 H, $J$ = 11.0 Hz), 2.01 (m, 2 H), 1.90 (m, 1 H, $J$ = 14.5, 7.5, 7.5, 7.5, 2.4 Hz), 1.77 (d, 1 H, $J$ = 14.6 Hz), 1.66 (m, 3 H), 1.59 (dd, 1 H, $J$ = 15.0, 5.2 Hz), 1.60 (m, 2 H), 1.47 (m, 1 H, $J$ = 14.3, 9.8, 7.3, 7.3, 7.3 Hz), 1.32 (s, 3 H), 1.33 (d, 3 H, $J$ = 6.4 Hz), 1.28 (d, 10 H), 1.25 (s, 3 H), 1.22 (d, 3 H, $J$ = 6.1 Hz), 1.20 (d, 3 H, $J$ = 7.6 Hz), 1.10 (d, 3 H, $J$ = 7.0 Hz), 1.09 (s, 3 H), 1.02 (d, 3 H, $J$ = 7.6 Hz), 0.92 (d, 3 H, $J$ = 6.4 Hz), 0.89 (t, 3 H, $J$ = 7.6 Hz), 0.88 (t, 3 H, $J$ = 7.0 Hz). $^{13}$C NMR (126 MHz, $CDCl_3$) [$\delta$/ppm]: 178.64 (s), 173.14 (s), 103.01 (s), 94.57 (s), 83. 79 (s), 77.98 (s), 77.81 (s), 77.40 (s), 74.11 (s), 73.63 (s), 73.50 (s), 72.93 (s), 71.13 (s), 69.99 (s), 68.67 (s), 65.51 (s), 65.01 (s), 62.38 (s), 51.84 (s), 49.31 (s), 45.16 (s), 42.20 (s), 41.88 (s), 38.29 (s), 36.71 (s), 36.58 (s), 36.16 (s), 34.59 (s), 31.64 (s), 29.77 (s), 29.28 (s), 28.98 (s), 27.42 (s), 26.86 (s), 26.68 (s), 25.79 (s), 22.52 (s), 21.88 (s), 21.51 (s), 21.18 (s), 21.14 (s), 18.13 (s), 16.10 (s), 14.64 (s), 14.00 (s), 11.14 (s), 9.21 (s), 7.25 (s). MS (ESI) $m/z$: 918.0 (calcd $[M + H]^+$ 918.0), purity 96%.

All other rationally designed compounds from training and validation set were prepared according to synthetic procedures described above (see Supporting Information).

Among commercially available macrolides, clarithromycin was purchased from US Pharmacopeia, roxithromycin and erythromycin were from Sigma, tylosin was from Wako Chemicals, and azithromycin was from PLIVA.

**Cells.** Primary cultures of normal human bronchial epithelial cells (NHBE, CC-2541, Lonza), normal human lung fibroblasts (NHLF, CC-2512, Lonza), and bronchial smooth muscle cells (BSMC, CC-2576, Lonza) were cultivated according to the protocols of the suppliers, and experiments were peformed while cells were between second and sixth passage. For the purpose of experiment, cells were seeded in 12-well plates and were used when they reached confluency.

NCI-H292 cells (ATCC, CRL-1848) were grown in RPMI 1640 medium (Gibco, Invitrogen) with 1% Glutamax (Gibco, Invitrogen), 10% fetal bovine serum (Biowest), and 1% sodium pyruvate (Gibco, Invitrogen). On the day before the experiment, cells were seeded in 12-well plates at a density of 4 × $10^5$ cells in 1.2 mL per well.

Human polymorphonuclear cells (PMN) and peripheral blood mononuclear cell (PBMC) from healthy volunteers were isolated from buffy coats. Erythrocytes were sedimented on 3% dextran T-500 (GE Healthcare), and leukocytes were separated by density gradient centrifugation on Ficoll-Paque PLUS

(GE Healthcare). PBMCs were collected and washed in phosphate buffered saline (PBS, Sigma). The pellets of PMNs were cleared from the residual erythrocytes by a brief hypotonic lysis and resuspended in RPMI 1640 medium.

Human T-lymphocytes (TLy) and monocytes were isolated from PBMCs on a magnetic separator (Vario MACS, Miltenyi Biotech) by negative selection using the Pan T Cell Isolation Kit II and Monocyte Isolation Kit II (Miltenyi Biotec), respectively, and resuspended in RPMI 1640 medium with 10% FBS. To obtain monocyte derived macrophages (MDM), monocytes were seeded in 12-well plates at a concentration of $1.5 \times 10^6$ cells/well in RPMI 1640 with 10% FBS and 5 ng/mL rhGM-CSF (R&D Systems) and cultured for the next 10 days with medium renewal every 2−3 days.

**Cellular Accumulation and Retention.** Cellular accumulation and retention experiments were performed as described by Bosnar et al.[9] with several adjustments. Compounds were dissolved in dimethylsulfoxide (DMSO) Hybri-Max (Sigma) at 20 mM. Cells were incubated with 3−20 $\mu$M macrolides in their corresponding culture medium for 3 h at 37 °C 5% $CO_2$ (for PMNs and NCI-N292 cells RPMI 1640 medium without FBS was used). To determine cellular accumulation, cells were then washed (PMNs by centrifugation through a layer of poly(dimethylsiloxane-*co*-diphenylsiloxane), dihydroxy terminated silicone oil (Aldrich); all other cells were washed three times with ice cold PBS) and lysed in 0.5% TritonX-100 (Sigma) in deionized water (Milli-Q, Millipore). To measure cellular retention of macrolides, after being washed, drug-loaded cells were incubated in fresh medium for 3 h. Cells were subsequently washed and lysed in 0.5% TritonX-100. All cell lysates were frozen, thawed, and centrifuged at 18000*g* for 10 min at +4 °C, and supernatants were collected and frozen until HPLC−MS/MS analysis.

Standards for the calibration curve were prepared by spiking lysates of drug-naive cells in 0.5% TritonX-100 with a series of known concentrations of the compound. Sample preparation for HPLC−MS/MS analysis was carried out as described previously.[45]

Analyses were performed by HPLC−MS/MS technique using Applied Biosystems API-2000 tandem MS, coupled with Agilent series 1100 binary pump and degasser and CTC PAL autosampler. The Phenomenex Luna 3 $\mu$m C18(2) 100A, 30 mm × 2.0 mm HPLC column and Phenomenex C18 4 mm × 2 mm guard column were used. Time program for mobile phases is in Supporting Information (Table S2). Tandem MS was set to MRM (multiple reaction monitor) mode. The instrument was tuned in positive mode (M+1−Q1 and most abundant fragment Q3). Internal standard (roxithromycin) was added to precipitation solution in order to compensate for possible injection volume errors and temperature related drifts.

Obtained macrolide concentrations were further normalized on total protein content in samples determined by the BCA method (Thermo Scientific). To minimize variation between donors, accumulations of compounds were expressed relative to the azithromycin value measured in each experiment with the azithromycin value set to 100%. Retention was expressed as a percentage of initially accumulated amount of compound that remained in cells after a 3 h washout period. Compounds were tested in triplicate samples (quadruplicate in PMNs) in two to five separate experiments, and mean values of all experiments were used in modeling.

**Physicochemical Measurements.** The aqueous acid ionization constants p$K_{a,i}$, the octanol−water partition coefficient (log $P_{o/w}$), and the distribution coefficient (log $D_{o/w}$ at pH 7.4) were measured by automated potentiometric titration using the instrument SiriusT3 (Sirius Analytical, Forest Row, East Sussex, U.K.). p$K_{a,i}$ values were also used for calculation of negative logarithm of the fraction of neutral (pNF) and charged (pCF_total) molecules present in aqueous solution at pH 7.4 as described by McFarland et al.[46]

Chromatographic hydrophobicity index (CHI) and CHI immobilized artificial membrane (IAM) values were determined using fast-gradient high-performance liquid chromatographic (HPLC) method and MS as a detector on the Waters early candidate profiling (ECP) four-way MUX LC/MS system (Waters Corp., U.K.). For the CHI[23] Luna C18(2) (Phenomenex, U.K.) HPLC columns were used while the CHI IAM[24] values were measured using Immobilized Artificial Membrane column with phosphatidylcholine (IAM PC DD column from Regis Analytical, West Lafayette, IL, U.S.) with fast acetonitrile gradient. The run time was 6 min including the re-equilibration of the stationary phases with the 50 mM pH 7.4 ammonium acetate buffer. CHI values were derived directly from a gradient reversed phase chromatographic retention time by using a calibration line obtained for standard compounds as described in the references (CHI,[23] CHI IAM[24]). The CHI value approximates to the volume % organic concentration when the compound elutes. CHI is linearly transformed into ChromlogD by least-squares fitting experimental CHI values to calculated ClogP values for over 20K research compounds using the following formula: ChromlogD = 0.0857 CHI − 2.00.

The DMSO precipitative solubility (Sol) and artificial membrane permeability (PERM) were measured by the in-house developed high-throughput (HT) methods with chemiluminesence nitrogen detection (CLND).[47] The DMSO enhanced, precipitative solubility measures how much compound from the starting 10 $\mu$L of 10 mM DMSO solution remained in solution after dilution with PBS buffer at pH 7.4 as described by Pan et al.[48] PERM measures how fast molecules (2.5 $\mu$L of 10 mM solution, pH 7.05) pass through a membrane, in this case phosphatidylcholine and cholesterol in *n*-decane solution (log $P_{app}$/nm/s).[49]

**Calculated Molecular Descriptors.** Calculated two-dimensional (2D) structural descriptors used in this study comprise the following: counts of H-bond donor (hbd) and acceptor (hba) atoms, count of positively charged atoms (POS), ratio of number of polar atoms (O, N, S) to number of carbon atoms (hetrat), atom-based E-state descriptors,[29]Abraham descriptors (solute excess molar refractivity (R2), dipolarity/polarizability (pi), summation hydrogen bond acidity (alpha), and basicity (beta), and the McGowan characteristic volume ($V_x$)).[30−32]

**Statistical Analysis.** Descriptive statistics and graphical analyses were done in JMP software for Windows, version 7 (1989−2007, SAS Institute Inc., Cary, NC) and SpotFire DecisionSite software, version 8.2.1 (2006, Spotfire, Inc., US, http://spotfire.tibco.com). Cross-correlation coefficients along with 95% confidence intervals were determined at http://faculty.vassar.edu/lowry/rho.html.

Continuous accumulation and retention values were analyzed by principal component analysis (PCA) and partial least-squares (PLS) techniques using SIMCA-P software, version 11.0 (Umetrics, Umeå, Sweden). Classification models were built using decision tree algorithm See5, version 11.0.0.0.[50] Prior to analysis the accumulation, retention and permeability values were transferred onto the $\log_{10}$ scale.

Categorical models were described by four statistics: total success, specificity, sensitivity, and Cohen's unweighted $\kappa$.[51] All four statistics should be close to 100% (or 1 for $\kappa$). Herein, compounds predicted as highly accumulated (retained) are defined as true positives (TP) if correctly predicted and as false positives (FP) if not correctly predicted by a model. Likewise, compounds forecasted as not low accumulated (retained) are either true negatives (TN) or false negatives (FN). Accordingly, total success is given by the formula (TP + TN)/(TP + TN + FP + FN) and represents a percentage of compounds accurately classified by a model. Sensitivity and specificity are calculated as TP/(TP + FN) and TN/(TN + FP), respectively. Sensitivity describes a model ability to identify actually accumulated/retained compounds, while specificity corresponds to a model ability to recognize only actual true negatives. Cohen's $\kappa$ value

represents a more robust model performance measure compared with the total success, since it takes into account the chance agreement. It was calculated at http://faculty.vassar.edu/lowry/kappa.html.

**Acknowledgment.** The study was supported by Glaxo-SmithKline Research Centre Zagreb, Croatia. The authors are thankful to Vesna Eraković Haber and Jasna Padovan for critical reading of the manuscript and Ksenija Štajcer on outstanding technical assistance in cellular PK experiments. The authors thank the members of Department of Chemistry and Department of Analytical Chemistry for their support. The modeling analyses performed by V.S. were partially supported through Grant 098-0982464-2511 (PI Dr. Koraljka Gall Trošelj), awarded by the Ministry of Science, Education and Sports of the Republic of Croatia.

**Supporting Information Available:** Experimental data, together with structures and structural characterization of all synthesized compounds within the training and validation set, as well as structures and literature references of their precursors; an Excel file containing Table S1 (xls format). This material is available free of charge via the Internet at http://pubs.acs.org.

## References

(1) Whitman, M. S.; Tunkel, A. R. Azithromycin and clarithromycin: overview and comparison with erythromycin. *Infect. Control Hosp. Epidemiol.* **1992**, *13*, 357–368.
(2) Culic, O.; Erakovic, V.; Parnham, M. J. Anti-inflammatory effects of macrolide antibiotics. *Eur. J. Pharmacol.* **2001**, *429*, 209–229.
(3) Shinkai, M.; Henke, M. O.; Rubin, B. K. Macrolide antibiotics as immunomodulatory medications: proposed mechanisms of action. *Pharmacol. Ther.* **2008**, *117*, 393–405.
(4) Hamada, K.; Mikasa, K.; Yunou, Y.; Kurioka, T.; Majima, T.; Narita, N.; Kita, E. Adjuvant effect of clarithromycin on chemotherapy for murine lung cancer. *Chemotherapy* **2000**, *46*, 49–61.
(5) Mikasa, K.; Sawaki, M.; Kita, E.; Hamada, K.; Teramoto, S.; Sakamoto, M.; Maeda, K.; Konishi, M.; Narita, N. Significant survival benefit to patients with advanced non-small-cell lung cancer from treatment with clarithromycin. *Chemotherapy* **1997**, *43*, 288–296.
(6) Andersen, S. L.; Oloo, A. J.; Gordon, D. M.; Ragama, O. B.; Aleman, G. M.; Berman, J. D.; Tang, D. B.; Dunne, M. W.; Shanks, G. D. Successful double-blinded, randomized, placebo-controlled field trial of azithromycin and doxycycline as prophylaxis for malaria in Western Kenya. *Clin. Infect. Dis.* **1998**, *26*, 146–150.
(7) Taylor, W. R.; Richie, T. L.; Fryauff, D. J.; Picarima, H.; Ohrt, C.; Tang, D.; Braitman, D.; Murphy, G. S.; Widjaja, H.; Tjitra, E.; Ganjar, A.; Jones, T. R.; Basri, H.; Berman, J. Malaria prophylaxis using azithromycin: a double-blind, placebo-controlled trial in Irian Jaya, Indonesia. *Clin. Infect. Dis.* **1999**, *28*, 74–81.
(8) Crosbie, P. A.; Woodhead, M. A. Long-term macrolide therapy in chronic inflammatory airway diseases. *Eur. Respir. J.* **2009**, *33*, 171–181.
(9) Bosnar, M.; Kelneric, Z.; Munic, V.; Erakovic, V.; Parnham, M. J. Cellular uptake and efflux of azithromycin, erythromycin, clarithromycin, telithromycin, and cethromycin. *Antimicrob. Agents Chemother.* **2005**, *49*, 2372–2377.
(10) Miossec-Bartoli, C.; Pilatre, L.; Peyron, P.; N'Diaye, E. N. Collart-Dutilleul, V.; Maridonneau-Parini, I.; Diu-Hercend, A. The new ketolide HMR3647 accumulates in the azurophil granules of human polymorphonuclear cells. *Antimicrob. Agents Chemother.* **1999**, *43*, 2457–2462.
(11) Wildfeuer, A.; Laufen, H.; Muller-Wening, D.; Haferkamp, O. Interaction of azithromycin and human phagocytic cells. Uptake of the antibiotic and the effect on the survival of ingested bacteria in phagocytes. *Arzneim.-Forsch.* **1989**, *39*, 755–758.
(12) Wildfeuer, A.; Reisert, I.; Laufen, H. Uptake and subcellular distribution of azithromycin in human phagocytic cells. Demonstration of the antibiotic in neutrophil polymorphonuclear leucocytes and monocytes by autoradiography and electron microscopy. *Arzneim.-Forsch.* **1993**, *43*, 484–486.
(13) Carlier, M. B.; Zenebergh, A.; Tulkens, P. M. Cellular uptake and subcellular distribution of roxithromycin and erythromycin in phagocytic cells. *J. Antimicrob. Chemother.* **1987**, *20* (Suppl. B), 47–56.
(14) Vazifeh, D; Abdelghaffar, H; Labro, M. T. Cellular accumulation of the new ketolide RU 64004 by human neutrophils: comparison with that of azithromycin and roxithromycin. *Antimicrob. Agents Chemother.* **1997**, *41*, 2099–2107.
(15) McDonald, P. J.; Pruul, H. Phagocyte uptake and transport of azithromycin. *Eur. J. Clin. Microbiol. Infect. Dis.* **1991**, *10*, 828–833.
(16) Amsden, G. W. Advanced-generation macrolides: tissue-directed antibiotics. *Int. J. Antimicrob. Agents* **2001**, *18* (Suppl. 1), S11–S15.
(17) Jain, R.; Danziger, L. H. The macrolide antibiotics: a pharmacokinetic and pharmacodynamic overview. *Curr. Pharm. Des.* **2004**, *10*, 3045–3053.
(18) Ganesan, A. The impact of natural products upon modern drug discovery. *Curr. Opin. Chem. Biol.* **2008**, *12*, 306–317.
(19) Gleeson, M. P. Generation of a set of simple, interpretable ADMET rules of thumb. *J. Med. Chem.* **2008**, *51*, 817–834.
(20) Leeson, P. D.; Springthorpe, B. The influence of drug-like concepts on decision-making in medicinal chemistry. *Nat. Rev. Drug Discovery* **2007**, *6*, 881–890.
(21) Mannhold, R; Poda, G. I.; Ostermann, C; Tetko, I. V. Calculation of molecular lipophilicity: State-of-the-art and comparison of log P methods on more than 96,000 compounds. *J. Pharm. Sci.* **2009**, *98*, 861–893.
(22) Girard, A. E.; Girard, D; English, A. R.; Gootz, T. D.; Cimochowski, C. R.; Faiella, J. A.; Haskell, S. L.; Retsema, J. A. Pharmacokinetic and in vivo studies with azithromycin (CP-62,993), a new macrolide with an extended half-life and excellent tissue distribution. *Antimicrob. Agents Chemother.* **1987**, *31*, 1948–1954.
(23) Valko, K.; Bevan, C.; Reynolds, D. Chromatographic hydrophobicity index by fast-gradient RP-HPLC: a high-throughput alternative to logP/logD. *Anal. Chem.* **1997**, *69*, 2022–2029.
(24) Valko, K.; Du, C. M.; Bevan, C. D.; Reynolds, D. P.; Abraham, M. H. Rapid-gradient HPLC method for measuring drug interactions with immobilized artificial membrane: comparison with other lipophilicity measures. *J. Pharm. Sci.* **2000**, *89*, 1085–1096.
(25) Djokic, S.; Kobrehel, G.; Lopotar, N.; Kamenar, B.; Nagl, A.; Mrvos, D. Synthesis and structure elucidation of 10-dihydro-10-deoxo-11-methyl-11-azaerythromycin A. *J. Chem. Res., Synop.* **1988**, 152–153.
(26) Morimoto, S.; Takahashi, Y.; Watanabe, Y.; Omura, S. Chemical modification of erythromycins. I. Synthesis and antibacterial activity of 6-*O*-methylerythromycins A. *J. Antibiot.* (*Tokyo*) **1984**, *37*, 187–189.
(27) Alihodzic, S.; Fajdetic, A.; Kobrehel, G.; Lazarevski, G.; Mutak, S.; Pavlovic, D.; Stimac, V.; Cipcic, H.; Kramaric, M. D.; Erakovic, V.; Hasenohrl, A.; Marsic, N.; Schoenfeld, W. Synthesis and antibacterial activity of isomeric 15-membered azalides. *J Antibiot.* (*Tokyo*) **2006**, *59*, 753–769.
(28) Culic, O.; Bosnar, M.; Marjanovic, N.; Jelic, D.; Alihodzic, S.; Vela, V.; Marusic-Istuk, Z.; Erakovic, V.; Bosnjak, B.; Hrvacic, B.; Tomaskovic, M.; Munic, V.; Ivetic, V.; Hutinec, A.; Kragol, G.; Leljak, M. Macrolides with Anti-Inflammatory Activity. WO 2006087644, 2006.
(29) Hall, L. H.; Kier, L. B.; Brown, B. B. Molecular similarity based on novel atom type electrotopological state indices. *J. Chem. Inf. Comput. Sci.* **1995**, *35*, 1074–1080.
(30) Abraham, M. H.; Chadha, H. S.; Martins, F.; Mitchell, R. C.; Bradbury, M. W.; Gratton, J. A. Hydrogen bonding. Part 46: A review of the correlation and prediction of transport properties by an LFER method: physicochemical properties, brain penetration and skin permeability. *Pestic. Sci.* **1999**, *55*, 78–88.
(31) Platts, J. A.; Abraham, M. H.; Butina, D.; Hersey, A. Estimation of molecular linear free energy relation descriptors using a group contribution approach. *J. Chem. Inf. Comput. Sci.* **1999**, *39*, 835–845.
(32) Zhao, Y. H.; Abraham, M. H.; Hersey, A.; Luscombe, C. N. Quantitative relationship between rat intestinal absorption and Abraham descriptors. *Eur. J. Med. Chem.* **2003**, *38*, 939–947.
(33) Hollosy, F.; Valko, K.; Hersey, A.; Nunhuck, S.; Keri, G.; Bevan, C. Estimation of volume of distribution in humans from high throughput HPLC-based measurements of human serum albumin binding and immobilized artificial membrane partitioning. *J. Med. Chem.* **2006**, *49*, 6958–6971.
(34) Lan, T; Rao, A; Haywood, J; Davis, C. B.; Han, C; Garver, E; Dawson, P. A. Interaction of macrolide antibiotics with intestinally expressed human and rat organic anion-transporting polypeptides. *Drug Metab. Dispos.* **2009**, *37*, 2375–2382.
(35) Valko, K. Application of high-performance liquid chromatography based measurements of lipophilicity to model biological distribution. *J. Chromatogr., A* **2004**, *1037*, 299–310.

(36) Yokogawa, K.; Ishizaki, J.; Ohkuma, S.; Miyamoto, K. Influence of lipophilicity and lysosomal accumulation on tissue distribution kinetics of basic drugs: a physiologically based pharmacokinetic model. *Methods Find. Exp. Clin. Pharmacol.* **2002**, *24*, 81–93.
(37) de Duve, C.; de Barsy, T.; Poole, B.; Trouet, A.; Tulkens, P.; Van, H. F. Commentary. Lysosomotropic agents. *Biochem. Pharmacol.* **1974**, *23*, 2495–2531.
(38) Trapp, S.; Rosania, G. R.; Horobin, R. W.; Kornhuber, J. Quantitative modeling of selective lysosomal targeting for drug design. *Eur. Biophys. J.* **2008**, *37*, 1317–1328.
(39) Duvvuri, M.; Krise, J. P. A novel assay reveals that weakly basic model compounds concentrate in lysosomes to an extent greater than pH-partitioning theory would predict. *Mol. Pharmaceutics* **2005**, *2*, 440–448.
(40) Moor, M. J.; Steiner, S. H.; Jachertz, G.; Bickel, M. H. Adipose tissue distribution and chemical structure of basic lipophilic drugs: desipramine, *N*-acetyl desipramine, and haloperidol. *Pharmacol. Toxicol.* **1992**, *70*, 121–124.
(41) Kaufmann, A. M.; Krise, J. P. Lysosomal sequestration of amine-containing drugs: analysis and therapeutic implications. *J. Pharm. Sci.* **2007**, *96*, 729–746.
(42) MacIntyre, A. C.; Cutler, D. J. The potential role of lysosomes in tissue distribution of weak bases. *Biopharm. Drug Dispos.* **1988**, *9*, 513–526.
(43) Bright, G. M.; Nagel, A. A.; Bordner, J.; Desai, K. A.; Dibrino, J. N.; Nowakowska, J.; Vincent, L.; Watrous, R. M.; Sciavolino, F. C.; English, A. R. Synthesis, in vitro and in vivo activity of novel 9-deoxo-9a-AZA-9a-homoerythromycin A derivatives; a new class of macrolide antibiotics, the azalides. *J. Antibiot.* (*Tokyo*) **1988**, *41*, 1029–1047.
(44) Mercep, M.; Mesic, M.; Tomaskovic, L.; Markovic, S.; Makaruha, O.; Poljak, V. Preparation of Steroid-Containing Macrolide Erythromycin Analog Glycosides for Treatment of Inflammatory Diseases. WO 2004005310, 2004.
(45) Munić, V; Kelnerić, Z; Mikac, L; Eraković Haber, V. Differences in assessment of macrolide interaction with human MDR1 (ABCB1, P-gp) using rhodamine-123 efflux, ATPase activity and cellular accumulation assays. *Eur. J. Pharm. Sci.* **2010**, *41*, 86–95.
(46) McFarland, J. W.; Berger, C. M.; Froshauer, S. A.; Hayashi, S. F.; Hecker, S. J.; Jaynes, B. H.; Jefson, M. R.; Kamicker, B. J.; Lipinski, C. A.; Lundy, K. M.; Reese, C. P.; Vu, C. B. Quantitative structure−activity relationships among macrolide antibacterial agents: in vitro and in vivo potency against *Pasteurella multocida*. *J. Med. Chem.* **1997**, *40*, 1340–1346.
(47) Bhattachar, S. N.; Wesley, J. A.; Seadeek, C. Evaluation of the chemiluminescent nitrogen detector for solubility determinations to support drug discovery. *J. Pharm. Biomed. Anal.* **2006**, *41*, 152–157.
(48) Pan, L.; Ho, Q.; Tsutsui, K.; Takahashi, L. Comparison of chromatographic and spectroscopic methods used to rank compounds for aqueous solubility. *J. Pharm. Sci.* **2001**, *90*, 521–529.
(49) Veber, D. F.; Johnson, S. R.; Cheng, H. Y.; Smith, B. R.; Ward, K. W.; Kopple, K. D. Molecular properties that influence the oral bioavailability of drug candidates. *J. Med. Chem.* **2002**, *45*, 2615–2623.
(50) Quinlan, J. R. *C4.5: Programs for Machine Learning*; Morgan Kaufmann Publishers, Inc.: San Mateo, CA, 1993.
(51) Cohen, J. Multiple regression as a general data-analytic system. *Psychol. Bull.* **1968**, *70*, 426–443.